NIH Public Access
Author Manuscript
Pain. Author manuscript; available in PMC 2012 April 1.

Published in final edited form as:
Pain. 2011 April ; 152(4): 912–923. doi:10.1016/j.pain.2011.01.016.

Inflammation alters trafficking of extrasynaptic AMPA receptors in tonically firing lamina II neurons of the rat spinal dorsal horn

Olga Kopach[a], **Sheng-Chin Kao**[b,c], **Ronald S. Petralia**[d], **Pavel Belan**[a], **Yuan-Xiang Tao**[b,*], and **Nana Voitenko**[a,*]

[a] Department of General Physiology of Nervous System, Bogomoletz Institute of Physiology, Kiev 01024, Ukraine

[b] Department of Anesthesiology and Critical Care Medicine, Johns Hopkins University School of Medicine, Baltimore, Maryland 21205, USA

[c] Department of Anesthesiology, Lin-Kou Medical Center, Chung Gung Memorial Hospital, Taoyaun County, Taiwan 333, ROC

[d] Laboratory of Neurochemistry, National Institute of Deafness and Other Communication Disorders, National Institutes of Health, Bethesda, Maryland 20892, USA

Abstract

Peripheral inflammation alters AMPA receptor (AMPAR) subunit trafficking and increases AMPAR Ca^{2+} permeability at synapses of spinal dorsal horn neurons. However, it is unclear whether AMPAR trafficking at extrasynaptic sites of these neurons also changes under persistent inflammatory pain conditions. Using patch-clamp recording combined with Ca^{2+} imaging and cobalt staining, we found that, under normal conditions, an extrasynaptic pool of AMPARs in rat substantia gelatinosa (SG) neurons of spinal dorsal horn predominantly consists of GluR2-containing Ca^{2+}-impermeable receptors. Maintenance of complete Freund's adjuvant (CFA)-induced inflammation was associated with a marked enhancement of AMPA-induced currents and $[Ca^{2+}]_i$ transients in SG neurons, while, as we previously showed, the amplitude of synaptically evoked AMPAR-mediated currents was not changed 24 h after CFA. These findings indicate that extrasynaptic AMPARs are upregulated and their Ca^{2+} permeability increases dramatically. This increase occurred in SG neurons characterized by intrinsic tonic firing properties, but not in those exhibited strong adaptation. This increase was also accompanied by an inward rectification of AMPA-induced currents and enhancement of sensitivity to a highly selective Ca^{2+}-permeable AMPAR blocker, IEM-1460. Electron microcopy and biochemical assays additionally showed an increase in the amount of GluR1 at extrasynaptic membranes in dorsal horn neurons 24 h post-CFA. Taken together, our findings suggest that CFA-induced inflammation increases functional expression and proportion of extrasynaptic GluR1-containing Ca^{2+}-permeable AMPARs in tonically firing excitatory dorsal horn neurons. We suggest that the altered extrasynaptic AMPAR trafficking might participate in the maintenance of persistent inflammatory pain.

*Corresponding authors: Dr. Nana Voitenko, Department of General Physiology of Nervous System, Bogomoletz Institute of Physiology, 4 Bogomoletz Str., Kiev 01024, Ukraine. Tel.:+38044-256-2049; Fax: +38044-256-2053; nana@biph.kiev.ua And Dr. Yuan-Xiang Tao, Department of Anesthesiology and Critical Care Medicine, Johns Hopkins University School of Medicine, 720 Rutland Ave., 370 Ross, Baltimore, MD 21205, USA. Tel: 443-287-5490; Fax: 410-502-5554; ytao1@jhmi.edu.

The authors declare no conflict of interests.

NIH-PA Author Manuscript
NIH-PA Author Manuscript
NIH-PA Author Manuscript

NIH-PA Author Manuscript

NIH-PA Author Manuscript

NIH-PA Author Manuscript

Keywords

Extrasynaptic AMPA receptors; GluR1 and GluR2 subunits; Peripheral inflammation; Receptor trafficking; Substantia gelatinosa neurons

1. Introduction

α-amino-3-hydroxy-5-methyl-4-isoxazolepropionic acid receptors (AMPARs) mediate fast excitatory transmission and play a critical role in synaptic plasticity in the central nervous system. AMPARs are present in multiple locations throughout neurons, including the extrasynaptic plasma membrane, where they have been identified within spines, dendrites, and somata. Numerous *in vitro* and *in vivo* studies have shown clearly that extrasynaptic AMPARs are highly mobile at the plasma membrane [8,38]. They rapidly move between the plasma membrane and intracellular compartments by exocytosis and endocytosis and can migrate laterally to and from synaptic sites [7,15,16]. Such receptor trafficking alters the number of synaptic AMPARs and might participate in synaptic plasticity under different cell conditions [8,13,44,47]. Extrasynaptic AMPARs can also contribute to glutamate-mediated signaling at nonsynaptic locations by responding to glutamate spillover or glial glutamate release [2,30,56]. Although it has been shown definitively that AMPARs are critically involved in activity-dependent changes of nociceptive inputs [23,28,41,54], most studies in this field have concentrated on elucidating the role of synaptic AMPARs, leaving possible involvement of extrasynaptic receptors open for consideration.

The functional properties of AMPARs, such as conduction and trafficking behavior, are determined by the subunit composition. AMPARs are heterotetramers composed of different combinations of the subunits GluR1 GluR4. Among these subunits, GluR1 and GluR2 are highly expressed in spinal dorsal horn. The ratio of GluR1/GluR2 determines Ca^{2+} permeability of AMPARs and rectification property of AMPAR-mediated currents in dorsal horn neurons [11,26,49]. Both Ca^{2+}-permeable and Ca^{2+}-impermeable AMPARs are expressed in substantia gelatinosa (SG) of the spinal cord, where primary afferents carrying nociceptive inputs to the spinal second-order neurons terminate [1,18,23,52]. In contrast to other parts of the central nervous system, a substantial proportion of SG neurons in adult rat dorsal horn densely express Ca^{2+}-permeable homomeric GluR1 AMPARs [1,9,18,23].

The changes in synaptic trafficking of AMPARs and their Ca^{2+}-permebility have been causally linked to multiple neuropathologic conditions, including excitotoxic vulnerability, neuronal injury [14,19,31,32], and persistent inflammatory pain [23,37,50]. It has been shown recently that neuroinflammatory factors promote lateral diffusion of GluR1/GluR2 heteromers from the extrasynaptic sites to synaptic sites, and enhance recycling of intracellular GluR1 homomers back to extrasynaptic membrane via exocytosis [19,32]. In spite of the functional significance of extrasynaptic AMPARs in modulation of spinal nociception, their trafficking during persistent inflammatory pain has not yet been studied.

Here we show that complete Freund's adjuvant (CFA)-induced inflammation causes an increase in functional expression of Ca^{2+}-permeable extrasynaptic AMPARs in rat SG neurons during the maintenance period of inflammatory pain. This increase occurred in neurons characterized by intrinsic tonic firing properties, but not in those that exhibited a strong adaptation. The change in AMPAR Ca^{2+} permeability might be related to a CFA-induced increase in GluR1 membrane insertion at extrasynaptic sites during the maintenance period of inflammatory pain.

NIH-PA Author Manuscript

NIH-PA Author Manuscript

NIH-PA Author Manuscript

2. Materials and Methods

2.1 Animal preparation

Male rats were housed in cages on a standard 12:12 h light/dark cycle. Water and food were available *ad libitum* until rats were transported to the laboratory for experiments. The animals were used in accordance with protocols that were approved by the Animal Care and Use Committee at the Bogomoletz Institute of Physiology and Johns Hopkins University and were consistent with the ethical guidelines of the National Institutes of Health and the International Association for the Study of Pain. All efforts were made to minimize animal suffering and to reduce the number of animals used.

2.2 Experimental drugs

CFA was purchased from Sigma Chemical Co. (St. Louis, MO). Fura-2 was obtained from Invitrogen (Carlsbad, CA, USA). Tetrodotoxin (TTX) was obtained from Alomone Labs Ltd. (Israel). CNQX, NBQX, APV, AMPA, SYM 2206, cyclothiazide (CTZ), GYKI 52466, bicuculline, strychnine, and 1-trimethylammonio-5-(1-adamantane-methyl-ammoniopentane dibromide) (IEM-1460) were purchased from Tocris Bioscience (Ellisville, MO).

2.3 Induction of peripheral inflammation

Persistent peripheral inflammation was induced in rats by injecting 100 μl of CFA (*Mycobacterium tuberculosis*) suspended in an oil-saline (1:1) emulsion subcutaneously into the plantar side of one hind paw. Because studies from our laboratory and those of others showed that CFA produces a significant change in synaptic AMPAR trafficking in dorsal horn neurons 24 h post-injection [41,42], we focused on this time point. Saline (0.9%; 100 μl) injection into age-matched rats was used as a control.

2.4 Spinal cord slice preparation

Spinal cord slices were prepared from 18- to 35-day-old male rats as described previously [41,54,57]. Briefly, after rats were deeply anesthetized with an overdose of isoflurane, the $L_{4–5}$ spinal segments were removed. Transverse slices (300 μm thick) were cut on a vibratome in an ice-cold solution containing (in mM) 250 sucrose, 2 KCl, 1.2 NaH_2PO_4, 0.5 $CaCl_2$, 7 $MgCl_2$, 26 $NaHCO_3$, 11 glucose (pH 7.4) and continuously bubbled with 95% O_2, 5% CO_2. Slices were maintained at room temperature (RT) in a physiologic Krebs bicarbonate solution that contained (in mM) 125 NaCl, 2.5 KCl, 1.25 NaH_2PO_4, 2 $CaCl_2$, 1 $MgCl_2$, 26 $NaHCO_3$, 10 glucose (pH 7.4, osmolarity 310–320 mOsM) and was equilibrated with 95% O_2, 5% CO_2.

2.5 Co^{2+} uptake labeling

The slices were labeled by Co^{2+} uptake as described previously [18]. Briefly, the slices from 25- to 35-day-old rats were transferred into a six-well plate containing oxygenated low-sodium and low-calcium Krebs solution containing (in mM) 50 NaCl, 2.5 KCl, 0.5 $CaCl_2$, 2 $MgCl_2$, 26 $NaHCO_3$, 25 glucose, and 135 sucrose at RT. This solution always contained 0.5 μM TTX and either 100 μM D-APV, 50 μM CNQX, or 50 μM GYKI 52466 or an equal volume of the appropriate vehicle (DMSO or saline). The stimulation solution was identical but also contained 250 μM kainate and 1.5 mM $CoCl_2$. After being exposed to the stimulation solution at RT for 20 min, slices were rinsed for 10 min in physiologic Krebs solution containing 5 mM EDTA to remove non-specifically bound Co^{2+}, and then for 5 min in physiologic Krebs solution. Cobalt ions were then precipitated by incubating the slices for 5 min in physiologic Krebs solution containing 0.12% $(NH_4)_2S$. Slices were rinsed again in physiologic Krebs solution and then fixed overnight in 4% paraformaldehyde in 0.1 M PBS at 4°C. They were cryoprotected in 30% sucrose in 0.1 M PBS and sectioned at a thickness

NIH-PA Author Manuscript

NIH-PA Author Manuscript

NIH-PA Author Manuscript

of 25 μm on a cryostat. Silver enhancement of cobalt precipitates was carried out as described [18].

Cobalt-labeled sections were quantified with an Olympus microscope (Olympus, Tokyo, Japan) linked to a Toshiba 3CCD camera (Toshiba, Japan) and I-Cube computer image analysis system (I-Cube, Cambridge, MA). The dorsal horn was divided into two regions: (1) the superficial laminae (laminae I and II) and (2) the nucleus proprius and neck of the dorsal horn (laminae III-VI). Five sections randomly selected from a total of 15 sections from each animal were analyzed. Two experimenters independently counted the number of Co^{2+}-labeled cells in two regions of the dorsal horn, with results that were consistent within 10%.

2.6 Immunohistochemistry

To define whether the Co^{2+}-labeled cells were neurons, some Co^{2+}-labeled sections were blocked for 1 h in PBS containing 10% goat serum and 0.3% TritonX-100 and then incubated with primary rabbit polyclonal antibody to NeuN (1:500, Chemicon, Temecula, CA) overnight at 4°C. Immunofluorescence histochemistry was carried out with goat anti-rabbit IgG conjugated with Rhodamine Red-X (1:300, Jackson ImmunoResearch, West Grove, PA). Control sections lacking primary antiserum were stained in parallel. All immunofluorescence-labeled sections were rinsed in 0.01 M PBS and mounted onto gelatin-coated glass slides. Cover slips were applied with a mixture of 50% glycerin and 2.5% triethylene diamine in 0.01 M PBS. The labeled sections were observed with an epifluorescence microscope under appropriate filter for Rhodamine Red-X (excitation 545–580 nm; emission ≥ 610 nm).

2.7 Synaptosomal membrane fraction

Biochemical fractionation was carried out according to previous studies with minor modification [48]. Briefly, 25–35-day-old rats were sacrificed by decapitation. The $L_{4–5}$ spinal segments ipsilateral to CFA (n = 4 rats) or saline (n = 4 rats) injection were collected. The dorsal part of the spinal cord was separated from the ventral part. The tissues were homogenized in homogenization buffer [in mM, 10 Tris-HCl (pH 7.4), 5 NaF, 1 sodium orthovanadate, 320 sucrose, 1 EDTA, 1 EGTA, 0.1 phenylmethylsulfonyl fluoride, 0.04 leupeptin, and 0.02 pepstatin A]. After centrifugation at 1,000 × *g* for 20 min at 4°C, the supernatant (S1, total soluble fraction) was collected and the pellet (P1, nuclei and debris fraction) discarded. The supernatant was centrifuged at 10,000 × *g* for 20 min to produce a pellet (P2) and supernatant (S2). The P2 was lysed hypo-osmotically in water and centrifuged at 25,000 × *g* to produce a pellet (P3). The S2 was considered to be the crude cytosolic fraction and the P3 the crude synaptosomal membrane fraction.

2.7 Surface biotinylation expression assay

Surface biotinylation expression experiments were performed in spinal cord slices as previously described [51]. Live transverse dorsal horn slices were prepared as described above from 25–35-day-old rats. Briefly, the slices were incubated with Krebs solution containing 1.5 mg/ml Sulfo-NHS-LC-biotin (Pierce, Rockford, IL) for 45 min on ice and rinsed in Krebs solution to quench the biotin reaction. The slices were homogenized in modified RIPA buffer (1% Triton X-100, 0.1% SDS, 0.5% deoxycholic acid, 50 mM $NaPO_4$, 150 mM NaCl, 2 mM NaF, 1 mM PMSF, 1 mg/ml leupeptin, 10 mM sodium pyrophosphate). The homogenates were centrifuged at 10,000 × *g* for 15 min at 4°C, and the supernatant was collected. After the measurement of protein concentration, 20% of the supernatant was removed to detect total expression of GluR1. The remaining supernatant was incubated with 50% NeutrAvidin agarose (Pierce) for 4 h at 4°C and washed three times

NIH-PA Author Manuscript

NIH-PA Author Manuscript

NIH-PA Author Manuscript

with RIPA buffer. Total and biotinylated surface proteins were detected by Western blotting analysis as described previously [40,41]. The surface/total ratio was calculated.

2.8 Postembedding immunogold labeling

Postembedding immunogold labeling was performed as described previously [25,41]. Briefly, 25–35-day-old rats were perfused transcardially with 4% paraformaldehyde + 0.5% glutaraldehyde 24 h after CFA or saline injection. Sections from ipsilateral L_5 superficial dorsal horn were cryoprotected and frozen in a Leica CPC cryopreparation chamber and freeze-substituted into Lowicryl HM-20 in a Leica AFS freeze substitution instrument. Thin sections were labeled with monoclonal mouse GluR2 and polyclonal rabbit GluR1, and controls were treated as described previously [25]. Areas for study were selected at random from the superficial dorsal horn at low magnification (i.e., synapses were not visible) and then micrographs of synapses were taken at high magnification. In the analyses, “synaptic” corresponded to the synaptic cleft and postsynaptic density, and “extrasynaptic” referred to the surface of the cell membrane to 20 nm deep and more than 100 nm from the edge of the active zone.

2.9 Simultaneous Ca^{2+} imaging and patch-clamp recording

Simultaneous Ca^{2+} imaging and whole-cell electrophysiological recordings were obtained from SG neurons of the spinal $L_{4–5}$ dorsal horn from 18–21-day-old rats as described previously [55]. Briefly, the neurons were visually identified with a video microscopy system (Olympus, Japan). The patch pipettes with resistance of 6–10 MΩ were filled with an internal solution containing (in mM) 133 K-gluconate, 5 NaCl, 0.5 $MgCl_2$, 10 HEPES-Na, 2 MgATP, 0.1 GTP-Na, and 0.2 fura-2 pentapotassium salt (pH 7.2, osmolarity 290 mOsM). The membrane potential of SG neurons was held at −60 mV by a patch-clamp amplifier PC-505B (Warner Instruments, Hamden, CT) and Digidata board 1320A (Molecular Devices, Union City, CA) controlled by pCLAMP 8.2 software (Axon Instruments, USA) in current or voltage-clamp mode. Only data from neurons that exhibited a resting membrane potential negative to −60 mV were included in the analysis.

SG neurons that were localized mainly in the mediolateral SG were chosen at random and categorized on the basis of their discharge pattern in response to a series of 1-s current pulses (Fig. 2). Of the 70 neurons tested, 35 were “tonically firing,” and 28 exhibited strong adaptation and were considered “transient” neurons. We also encountered a few neurons that exhibited a sustained delay prior to the action potential’s discharge or that discharged action potentials followed by firing accommodation. We characterized those neurons as transient if the number of spikes was dependent on the pulse strength, and the neuron exhibited an adaptation when the applied depolarizing current (20–30 pA) was increased [36,46]. Other unclassified neurons that were not characterized by any aforementioned categories were excluded from the analysis.

To isolate the AMPAR-mediated membrane current and the associated $[Ca^{2+}]_i$ increase, recordings were made in the continuous presence of D-APV (50 μM), bicuculline (5 μM), and strychnine (2 μM) to block NMDA, $GABA_A$, and glycine receptors respectively. In addition, TTX (0.5 μM) and cadmium chloride (100 μM) were added to Krebs bicarbonate solution to block corresponding voltage-activated sodium and calcium channels. To prevent a desensitization of AMPARs during bath application of agonist to slices, AMPA was applied in the continuous presence of CTZ (20 μM). Typically, one neuron was studied per slice. Simultaneous fura-2 fluorescence was measured by using a 60× water-immersion objective and a 12-bit cooled CCD camera and capturing board (Sensicam, PCO, Germany). Fluorescent signals from SG neurons were collected between 50 and 100 μm below the surface of the slice. Calcium changes were detected by a PolyChrome IV monochromator

NIH-PA Author Manuscript

NIH-PA Author Manuscript

NIH-PA Author Manuscript

(Till Photonics, Germany) as the change in fluorescence of fura-2 dye measured at wavelengths > 510 nm when excitation light was 380 nm. The monochromator was attenuated with neutral density filters to avoid bleaching of fura-2. Imaging Workbench software (INDEC System, USA) was used to measure changes in fura-2 fluorescence. When AMPA was applied exogenously to SG neurons, fluorescence changes in soma and dendrites were measured simultaneously and expressed as changes in the ratio of fura-2 fluorescence at 340 and 380 nm, which is proportional to $[Ca^{2+}]_i$. The background closest to the area of interest was subtracted. The amplitude of AMPA-induced $[Ca^{2+}]_i$ signal was estimated as the difference between the fura-2 fluorescence ratio prior to AMPA application and that at the maximum $[Ca^{2+}]_i$ rise after AMPA stimulation.

To study the current-voltage (*I-V*) relationship, we recorded membrane currents using an internal solution that contained (in mM) 130 Cs-methylsulphonate, 10 NaCl, 0.5 EGTA, 10 HEPES, 0.2 spermine tetrahydrochloride, 2 Mg-ATP, and 0.1 Na-GTP; pH was adjusted to 7.2 with CsOH (osmolarity 290 mOsM) at RT. *I-V* curves were constructed by holding neurons at −70 mV in a voltage clamp and ramping for 100–300 ms every 5 s initially to +50 mV and then to −70 mV. We applied short hyperpolarizing voltage steps to −75 mV before every ramp to monitor input and access resistance. To inhibit K^+-channel currents, we recorded the AMPA-induced currents after at least 10 min perfusion of patched neurons with an internal solution. To isolate the extrasynaptic AMPAR-mediated current, we subtracted the ramp currents recorded before AMPA application from the currents recorded during the bath AMPA application at each membrane potential. The rectification index (RI) of the extrasynaptic AMPAR-mediated current was determined by dividing the AMPA-induced current amplitude at +30 mV by the current amplitude at −50 mV.

To block Ca^{2+}-permeable AMPARs, we used IEM-1460 which was applied before (3–5 min) or after establishing the steady-state level of AMPA-induced current.

2.10 Statistical analysis

All data are presented as mean ± SEM with *n* referring to the number of cells analyzed. Student's t-tests (two-tailed unpaired) were used to determine statistically significant differences. A *p* value of less than 0.05 was considered as statistically significant.

3. Results

3.1 Peripheral inflammation increases AMPAR-mediated Ca^{2+}-permeability in dorsal horn neurons

Kainate-induced cobalt uptake has been used to visualize Ca^{2+}-permeable AMPARs in dorsal horn neurons [18]. To determine whether CFA-induced peripheral inflammation alters the expression of spinal Ca^{2+}-permeable AMPARs, we analyzed kainate-induced cobalt uptake in spinal cord transverse slices derived from adult rats (25–35 days) 24 h after saline or CFA injection. Although the dorsal horns of adult saline-treated rats contained fewer cobalt-positive cells than those of younger naïve rats (P6-14) [18,23], their patterns of cobalt uptake were similar (Fig. 1A). Cobalt-positive cells were predominantly observed in laminae I and II; few were distributed in laminae III–VII (Fig. 1A). To assess whether this pattern reflected selective cobalt uptake through AMPARs, we pre-incubated the slices with GYKI 52466, CNQX, or APV. AMPAR antagonists, CNQX and GYKI 52466 entirely abolished kainate-induced cobalt uptake in the slices, whereas NMDAR antagonist APV had no effect (Fig. 1A). To determine whether kainate-induced cobalt uptake occurred in neurons rather than in other cell types, we incubated the sections with a primary antibody against neuronal marker NeuN after kainate-induced cobalt uptake. In the dorsal horn, most cells that took up cobalt (90 ± 7%, n = 4) were positive for NeuN (Fig. 1B). We found that

NIH-PA Author Manuscript

NIH-PA Author Manuscript

NIH-PA Author Manuscript

CFA (but not saline) injection significantly increased cobalt uptake loading in dorsal horn on the ipsilateral, but not contralateral, side (Fig. 1C). After 24 h, the number of cobalt-positive cells was 2.77-fold greater ($p < 0.01$, n = 4) in laminae I–II and 3.73-fold greater ($p < 0.01$, n = 4) in laminae III VII of CFA-injected rats than in those regions of saline-treated rats (Fig. 1D). However, some NeuN-labeled cells in the superficial and deep dorsal horn were still not cobalt-positive (Fig. 1C), indicating that this group of dorsal horn neurons fails to alter AMPAR Ca^{2+} permeability in response to peripheral inflammatory stimulation.

3.2 Peripheral inflammation augments extrasynaptic AMPAR-mediated currents and $[Ca^{2+}]_i$ transients in "tonic" but not in "transient" lamina II neurons

The fact that a CFA-induced increase in cobalt uptake was observed predominantly in neuronal bodies of dorsal horn suggests that Ca^{2+}-permeable AMPARs are upregulated in dorsal horn neurons during CFA-induced peripheral inflammation. By simultaneously recording AMPA-induced membrane current and associated $[Ca^{2+}]_i$ changes in soma and dendrites of superficial lamina II neurons of the spinal $L_{4–5}$ dorsal horn, we directly evaluated upregulation of AMPARs and their Ca^{2+} permeability 24 h after saline or CFA injection. According to intrinsic firing properties during sustained membrane depolarization, lamina II neurons were predominantly divided into two groups: "tonic" and "transient" (Fig. 2). Tonic neurons (n = 35) were defined as those able to support continued discharge of action potentials during 1-s depolarizing inward current and an increased frequency of discharge with increasing current intensity (Fig. 2C). Transient neurons (n = 28) were those that exhibited a strong adaptation by generating short bursts of spikes or just a single spike regardless of depolarizing current intensity (Fig. 2D). Tonic and transient neurons demonstrated similar changes in $[Ca^{2+}]_i$ after depolarizing inward currents (Fig. 2E, F), indicating that the contribution of voltage-gated Ca^{2+} channels to spike generation was similar in the two groups.

To activate the total pool of AMPARs and mimic excessive glutamate release from presynaptic neurons and glia during dorsal horn injuries or inflammation [2,30,56], we bath applied AMPA to the slices. Bath administration of AMPA (5 μM, 60 s) evoked an inward current at a holding potential of −60 mV in both tonic and transient neurons (Fig. 3A, bottom trace). It was characterized by a slow rising phase and desensitization to a plateau level. This current is predominantly mediated by extrasynaptic AMPARs due to their relative abundance compared to synaptic ones in the neuronal plasma membrane [3,22]. No significant difference was observed between the amplitudes of the AMPA-induced currents in the tonic (−204 ± 18 pA, n = 35) and transient (−173 ± 19 pA, n = 28) neurons (Fig. 3D; $p = 0.24$). The current activation was associated with a synchronous rise in $[Ca^{2+}]_i$ in both the soma and dendrites in all examined neurons (Fig. 3A, upper traces). A typical calcium response to AMPA application consisted of a fast initial transient rise in $[Ca^{2+}]_i$ followed by a slow decay to the baseline within several minutes. A comparison of $[Ca^{2+}]_i$ transient amplitudes, expressed as an increase in the ratio of fura-2 fluorescence at 340 and 380 nm, ΔR (see Methods), showed no significant differences in the amplitudes between tonic and transient groups of neurons. Average amplitudes of AMPA-induced $[Ca^{2+}]_i$ transients were 0.47 ± 0.10 (n = 21, tonic) vs 0.48 ± 0.09 (n = 22, transient; $p > 0.1$) for soma and 0.60 ± 0.12 (n = 14, tonic) vs 0.52 ± 0.09 (n = 18, transient; $p > 0.1$) for dendrites (Fig. 3D). These findings indicate that the two groups of neurons have similar levels of AMPAR expression.

The observed AMPA-induced currents and $[Ca^{2+}]_i$ transients were mediated by AMPAR activation, as NBQX, a non-selective AMPAR antagonist, and GYKI 52466, a selective AMPAR antagonist, significantly inhibited the currents. NBQX inhibited AMPA-induced current amplitudes by 97 ± 9% (n = 3, $p < 0.0001$) and 98 ± 11% (n = 3, $p < 0.0001$) in tonic and transient neurons, respectively. GYKI 52466 inhibited the amplitudes by 75 ± 15% (n = 5, $p < 0.05$) and by 86 ± 15% (n = 7, $p < 0.01$) in the tonic and transient neurons,

NIH-PA Author Manuscript

NIH-PA Author Manuscript

NIH-PA Author Manuscript

respectively. NBQX inhibited somatic and dendritic $[Ca^{2+}]_i$ transients in tonic neurons by 93 ± 20% and 88 ± 12%, respectively (n = 3, $p < 0.05$) and somatic $[Ca^{2+}]_i$ transients in transient neurons by 92 ± 17% (n = 3, $p < 0.05$). GYKI 52466 inhibited somatic and dendritic $[Ca^{2+}]_i$ transients in tonic neurons by 94 ± 20% (n = 5, $p < 0.05$) and 92 ± 18% (n = 5, $p < 0.01$), respectively, and inhibited somatic and dendritic $[Ca^{2+}]_i$ transients of the transient group by 83 ± 15% (n = 3, $p < 0.05$) and 92 ± 15% (n = 3, $p < 0.05$), respectively.

CFA-induced inflammation significantly increased AMPA-induced currents and associated $[Ca^{2+}]_i$ transients in tonically firing group of neurons (Fig. 4A, B, D). The amplitude of AMPA-induced inward current was increased by 125 ± 13% (n = 20; $p < 0.001$) 24 h post-CFA compared to post-saline (Fig. 4A, D). The increase in AMPA-induced current was associated with an augmentation in amplitudes of somatic and dendritic $[Ca^{2+}]_i$ transients. Twenty-four hours after CFA injection, the amplitude of $[Ca^{2+}]_i$ transients increased by 92 ± 11% and 96 ± 17% in soma and dendrites, respectively (n = 11; $p < 0.05$; average amplitude in soma: 0.47 ± 0.10 post-saline vs 0.91 ± 0.10 post-CFA; average amplitude in dendrites: 0.60 ± 0.12 post-saline vs 1.17 ± 0.21 post-CFA; Fig. 4A, D). At the same time, we found no significant differences between the tonic neurons from the saline-and CFA-treated animals in electrophysiological properties such as input resistance (saline: 612 ± 111 MΩ, n = 25; CFA: 604 ± 75 MΩ, n = 25. $p > 0.5$), capacitance (saline: 22 ± 1 pF, n = 26; CFA: 24 ± 1 pF, n = 30. $p = 0.2$) as well as a series resistance (saline: 28 ± 2 MΩ, n = 25; CFA: 30 ± 2 MΩ, n = 25. $p = 0.4$). These findings clearly indicate a marked increase in functional expression of AMPARs in the dendrites and soma of tonically firing SG neurons during the maintenance of persistent inflammation. The data from our laboratory [41] and those of others [28,54] have demonstrated that CFA-induced inflammatory input does not significantly alter the amplitude of synaptically evoked AMPAR-mediated excitatory postsynaptic currents (eEPSCs) in the superficial dorsal horn neurons at 24 h post-CFA. Thus, the increase in AMPA-induced currents in the tonically firing SG neurons that we observed after inflammation can be attributed to upregulation of an extrasynaptic pool of AMPARs. In addition, a marked increase in the amplitudes of $[Ca^{2+}]_i$ transients suggests that this upregulation of AMPA-induced current is accounted for by an increase in the number of extrasynaptic Ca^{2+}-permeable AMPARs.

Interestingly, CFA-induced inflammation did not produce significant changes in AMPAR-mediated currents and associated somatic and dendritic $[Ca^{2+}]_i$ transients in transient neurons. The amplitudes of AMPA-induced currents were 173 ± 19 pA in the saline-treated group (n = 28) and 150 ± 17 pA in the CFA-treated group (n = 21; $p > 0.37$; Fig. 4C, D). The amplitudes of AMPA-induced $[Ca^{2+}]_i$ transients in soma were 0.48 ± 0.09 (n = 21) and 0.47 ± 0.08 (n = 8) in the saline- and CFA-treated groups, respectively ($p > 0.9$; Fig. 4D). The amplitudes of AMPA-induced $[Ca^{2+}]_i$ transients in dendrites were 0.52 ± 0.09 (n = 18) and 0.59 ± 0.1 (n = 6) in the saline- and CFA-treated groups, respectively ($p > 0.6$; Fig. 4D). Additionally, inflammation did not significantly change series resistance (saline: 27 ± 1 MΩ, n = 38; CFA: 29 ± 1 MΩ, n = 32. $p = 0.2$), input resistance (saline: 682 ± 92 MΩ, n = 38; CFA: 663 ± 91 MΩ, n = 37. $p > 0.5$), or capacitance (saline: 17 ± 2 pF, n = 38; CFA: 19 ± 1 pF, n = 37. $p = 0.5$) in the transient neurons. These results indicate that the total pool of extrasynaptic and synaptic AMPARs in dendrites and somata was not changed in the transient group of SG neurons during maintenance of persistent inflammation.

3.3 Peripheral inflammation increases the proportion of Ca^{2+}-permeable AMPARs in the total pool of extrasynaptic AMPARs

Persistent inflammation changes a proportion of Ca^{2+}-permeable AMPARs to Ca^{2+}-impermeable AMPARs at synapses in dorsal horn neurons during the maintenance period of CFA-induced inflammatory pain [28,41,54]. To establish whether inflammation also changes this parameter for extrasynaptic populations of AMPARs, we first examined the

NIH-PA Author Manuscript

NIH-PA Author Manuscript

NIH-PA Author Manuscript

effect of selective Ca^{2+}-permeable AMPAR blocker on AMPA-induced currents. IEM-1460, a polyamine derivative, rapidly and reversibly blocks Ca^{2+}-permeable AMPARs [10]. In the saline-treated rats, IEM-1460 (40 μM) produced a small, insignificant effect on amplitudes of AMPA-induced currents when it was applied to slices before AMPA (5–7 min, Fig. 5A, left graph) or when it was applied during a steady-state period of AMPA-induced current (Fig. 5A, right graph). In tonic neurons from the saline-treated group, the inhibitory effect of IEM-1460 on AMPA-induced current amplitude was small and insignificant (7 ± 2%, n = 7; $p > 0.45$; Fig. 5B), indicating that Ca^{2+}-permeable extrasynaptic AMPARs only slightly contribute to the total AMPA-induced current under normal conditions. On the contrary, sensitivity of synaptic AMPAR-mediated eEPSCs in SG neurons to Ca^{2+}-permeable AMPAR blockers was substantially greater (~23% inhibition [41,54]), further indicating that synaptic AMPARs do not contribute substantially to the generation of AMPA-induced currents. In contrast, in the CFA-treated group, the inhibitory effect of IEM-1460 on AMPA-induced current amplitude was substantially enhanced in the tonic neurons (26 ± 5%; n = 10; $p < 0.01$, Fig. 5A, B). This finding suggests that persistent peripheral inflammation not only increases the number of Ca^{2+}-permeable AMPARs at extrasynaptic sites in the tonic SG neurons but also increases their proportion in the total pool of extrasynaptic AMPARs. IEM-1460 had no significant effect on the amplitude of AMPA-induced current in the transient neurons from saline- or CFA-treated groups (saline: 7 ± 3%, n = 5, CFA: 15 ± 5%, n = 5, $p = 0.22$, Fig. 5B).

The proportion of extrasynaptic Ca^{2+}-permeable AMPARs in the somatic and dendritic pools was also examined based on the unique rectification properties of AMPAR-mediated currents. To obtain an *I-V* relationship of the AMPA-induced currents, we held neurons at −70 mV and ramped every 5 s initially to +50 mV and then to −70 mV before and during bath application of AMPA (Fig. 5C, upper panel). To isolate an AMPAR-mediated component of a current, we subtracted the ramp currents recorded before AMPA application from those recorded during the agonist application (see Methods for details). In the tonic neurons, the *I-V* curves showed weak rectification at positive membrane potentials in the saline-treated group that differed from the strong rectification of synaptic eEPSCs [41]. However, a significant inward rectification was observed in the CFA-treated group (Fig. 5C). To estimate the rectification of AMPA-induced currents, we calculated a rectification index expressed as a ratio of the current amplitudes at positive and negative membrane potentials ($RI_{+30/-50}$). RI was 0.74 ± 0.07 (n = 11) in the saline-treated group and 0.27 ± 0.05 (n = 12; $p < 0.001$, Fig. 5D) in the CFA-treated group. In contrast, RI for synaptic AMPAR-mediated eEPSCs was 0.26 and 0.18 in SG neurons from saline-treated and CFA-inflamed rats, respectively [41], further confirming that synaptic and extrasynaptic AMPA receptors have different properties.

CFA-induced inward rectification of AMPA-induced currents could be reversed by IEM-1460 (Fig. 5C). The RI value was significantly increased to 0.91 ± 0.05 after IEM-1460 treatment (n = 5; $p < 0.001$, Fig. 5D, E). These findings further indicate an increased proportion of extrasynaptic Ca^{2+}-permeable AMPARs in dorsal horn neurons during the maintenance of peripheral inflammation.

3.4 Peripheral inflammation induces GluR1 membrane insertion at extrasynaptic sites of dorsal horn neurons

To further validate whether extrasynaptic Ca^{2+}-permeable AMPARs are increased in plasma membrane of dorsal horn neurons under persistent inflammatory conditions, we used a combined approach of post-embedding immunogold labeling with electron microscopy (EM) to compare ultrastructural distribution of GluR1 and GluR2 in superficial dorsal horn 24 h after saline (n = 2) or CFA (n = 2) injection. We focused on these two subunits because they are more abundant in dorsal horn than are GluR3 and GluR4 [9,18,29]. We counted the

NIH-PA Author Manuscript

NIH-PA Author Manuscript

NIH-PA Author Manuscript

immunogold-labeled particles at synapses, in extrasynaptic membranes, and in cytoplasm in both saline- and CFA-treated groups. Consistent with previous reports [41,43], we observed GluR1 and GluR2 immunogold labeling in postsynaptic membranes, cytoplasm, and extrasynaptic membranes in the saline-treated group (Fig. 6A). CFA injection produced a tendency toward an increase in the number of GluR1-labeled particles in extrasynaptic membranes and a decrease in synaptic membranes and cytoplasm (Fig. 6B). The ratio of the number of GluR1-labeled particles in the CFA-treated group to the number in the saline-treated group was 0.62 at synapses, 2.54 at extrasynaptic membranes, and 0.79 in the cytoplasm (n = 57; Fig. 6B). In agreement with our previous report [41], CFA injection led to a decrease in the number of GluR2-labled particles at synapses and a tendency toward an increase in the cytoplasm (Fig. 6B). The ratio of the number of GluR2-labeled particles in the CFA-treated group to the number in the saline-treated group was 0.61 at synapses, 1.05 at extrasynaptic membranes, and 1.2 in the cytoplasm (n = 47; Fig. 6B). These findings indicate that peripheral inflammation might induce GluR1 membrane insertion at extrasynaptic membranes and GluR2 internalization at synapses in superficial dorsal horn.

EM immunogold study of low-density extrasynaptic receptors has spatial and sample size limitations. To further confirm our observation, we used a surface biotinylation expression assay and synaptosomal fractionation approach to compare the expression of GluR1 in surface plasma membranes and in synaptic membranes derived from the dorsal horn. For the surface biotinylation expression assay, live slices were prepared from the ipsilateral $L_{4–5}$ dorsal horn 24 h after saline (n = 4) or CFA (n = 4) injection. The surface receptors were labeled with biotin and then precipitated [41,51]. The amount of surface GluR1 was 33% greater in the CFA-treated group than in the saline-treated group ($p < 0.05$) (Fig. 7A). In control experiments, β-actin, an intracellular protein, could not be precipitated by biotin (Fig. 7A). Using differential centrifugation [49], we collected synaptosomal fractions that contained abundant synaptic receptors from the ipsilateral $L_{4–5}$ dorsal horn tissues 24 h after saline (n = 4) or CFA (n = 4) injection. Western blot analysis showed that the level of GluR1 in the synaptosomal fraction of the CFA-treated group was similar to that of the saline-treated group ($p > 0.05$; Fig. 7B). Taken together, our findings suggest that the amount of GluR1 in extrasynaptic membranes is increased in dorsal horn under persistent inflammatory conditions.

4. DISCUSSION

In the present study, we have demonstrated that peripheral inflammation markedly increases the absolute number of, as well as the proportion of Ca^{2+}-permeable AMPARs in the extrasynaptic membrane of tonically firing SG neurons during the maintenance period of inflammatory pain. Our morphological and biochemical results further showed increased membrane insertion of extrasynaptic GluR1 at 24 h post-CFA. This inflammation-associated increase in functional expression of extrasynaptic GluR1-containing Ca^{2+}-permeable AMPARs in the tonically firing dorsal horn neurons might contribute to the maintenance of persistent inflammatory pain.

4.1 Composition of extrasynaptic AMPARs under normal conditions

A high level of extrasynaptic AMPAR immunoreactivity has been detected throughout the central nervous system, including the dorsal horn [39–42]. By using electrophysiological, imaging, and immunochemical approaches, we demonstrated the presence of functional AMPARs at extrasynaptic sites of dorsal horn neurons. Their functional properties are distinct from those of synaptic AMPARs [28,41,52,54]. AMPA-induced currents in the neurons of naive rats displayed roughly linear current-voltage relationships (RI = 0.74) and were not significantly suppressed by the specific Ca^{2+}-permeable AMPAR blocker IEM-1460 (Fig. 5). In contrast, we observed that AMPAR-mediated EPSCs (RI = 0.26) had

NIH-PA Author Manuscript

NIH-PA Author Manuscript

NIH-PA Author Manuscript

prominent rectification and were substantially inhibited by polyamine blockers (23%) [41]. These findings suggest that receptors with synaptic AMPAR properties did not significantly contribute to AMPA-induced currents, which were mediated mainly by AMPARs located at extrasynaptic sites. These results also indicate that most extrasynaptic AMPARs in SG neurons consist of GluR2 subunits and are Ca^{2+}-impermeable under normal conditions. Consistently, immunogold labeling showed more GluR2 than GluR1 in the extrasynaptic profiles of the superficial dorsal horn neurons (Fig. 6B). At the same time, the AMPA-induced currents did evoke $[Ca^{2+}]_i$ transients, implying that a minor proportion of Ca^{2+}-permeable AMPARs are located in the plasma membrane of SG neurons (Fig. 3). Our findings indicate that GluR2-containing Ca^{2+}-impermeable AMPARs are dominant at extrasynaptic sites in normal superficial dorsal horn. Similar differences in synaptic and extrasynaptic AMPAR channel composition have been reported in other brain regions [6,35].

4.2 Trafficking of extrasynaptic AMPARs during persistent pain

Extrasynaptic AMPAR trafficking in dorsal horn during inflammatory pain has not been well studied. Previous studies have shown that persistent inflammation induces synaptic GluR2 internalization. This internalization results in a switch from Ca^{2+}-impermeable to Ca^{2+}-permeable AMPAR-mediated neurotransmission at synapses in dorsal horn, although the amplitude of eEPSCs was not changed [28,41,54]. In the present study, we found a significant increase in the amplitudes of AMPAR-mediated current (evoked by bath application of AMPA) and the associated $[Ca^{2+}]_i$ transients recorded in soma and dendrites of the tonically firing SG neurons at 24 h post-CFA (Fig. 4). These data indicate that the number of extrasynaptic Ca^{2+}-permeable AMPARs is substantially increased in the tonic SG neurons after inflammation. Moreover, the *I-V* curves obtained in SG neurons from rats with peripheral inflammation were inwardly rectified, and sensitivity to the selective inhibition of Ca^{2+}-permeable AMPARs was significantly increased at 24 h post-CFA (Fig. 6). Our results indicate that peripheral inflammation might increase the number of Ca^{2+}-permeable AMPARs at extrasynaptic sites as well as the proportion of them in the total pool of extrasynaptic AMPARs in dorsal horn neurons during the maintenance period. In line with these results, previous studies have demonstrated that the amount of GluR1 was increased (by 23%) and that the amount of GluR2 was correspondingly decreased (by 25%) in the crude membrane fraction of ipsilateral dorsal horn 1 day after intraplantar CFA injection [28,42]. In the present study, we also showed that surface membrane expression of GluR1 in dorsal horn from the CFA-treated group was 33% greater than that in the saline-treated group (Fig. 7A). Since we found no significant difference in the levels of GluR1 in the synaptosomal fraction of the ipsilateral dorsal horn between the CFA- and saline-treated groups (Fig. 7B), the observed increase in surface membrane GluR1 mostly reflects an increase in the extrasynaptic pool of receptors. Our findings suggest that persistent inflammation promotes marked insertion of GluR1-containing Ca^{2+}-permeable AMPARs at extrasynaptic membrane sites. The data from our laboratory and those of others [28,41] showed that the amount of GluR2 decreased at surface plasma membranes and synapses while correspondingly increasing in the cytoplasm in dorsal horn at 24 h post-CFA. Therefore, it is evident that peripheral inflammation might produce a reciprocal rearrangement of GluR1-containing Ca^{2+}-permeable and GluR2-containing Ca^{2+}-impermeable AMPARs in different cellular pools of dorsal horn neurons.

4.3 Functional significance of increased extrasynaptic Ca^{2+}-permeable AMPARs

Our findings suggest that persistent inflammatory insult alters trafficking of extrasynaptic AMPARs in dorsal horn and induces delivery of spinal GluR1-containing Ca^{2+}-permeable AMPARs to extrasynaptic sites. Although it is well established that Ca^{2+}-permeable AMPARs facilitate nociceptive plasticity and enhance long-lasting inflammatory

NIH-PA Author Manuscript

NIH-PA Author Manuscript

NIH-PA Author Manuscript

hyperalgesia [23,27,37], molecular mechanisms that underlie these events are still unclear. Surface AMPARs represent a mobile population that traffics between synaptic and extrasynaptic sites [24]. Since the extrasynaptic AMPARs are subjected to Brownian-like unrestricted mobility, the dynamic equilibrium between synaptic and extrasynaptic receptor pools determines the number of synaptic receptors and synaptic strength [53]. We found that inflammatory insult promotes insertion of GluR1-containing Ca^{2+}-permeable AMPARs at extrasynaptic membranes. These extrasynaptic Ca^{2+}-permeable receptors can diffuse laterally in the plasma membrane to the postsynaptic density [17] where they might be trapped at synapses [41,50]. It is very likely that an inflammation-induced increase in extrasynaptic Ca^{2+}-permeable AMPARs may be involved in the mechanisms that underlie a persistent increase in synaptic Ca^{2+}-permeable AMPARs in the dorsal horn neurons that has been reported recently [28,41,54]. Persistent inflammatory insult also induces PKC-dependent disruption of GluR2 binding to its synaptic anchoring proteins [4], promotes GluR2 internalization from synapses, and decreases the number of synaptic GluR2-containing AMPARs [28,41,54]. All of these events finally result in an increase of synaptic [28,41,54] and extrasynaptic AMPAR Ca^{2+} permeability. This conclusion is supported by inflammation-induced potentiation of $[Ca^{2+}]_i$ transients evoked in SG neurons by dorsal root stimulation [37,55]. The related increase in intracellular Ca^{2+} concentration should initiate or potentiate a variety of Ca^{2+}-dependent intracellular cascades that are associated with the mechanisms of pain hypersensitivity during inflammatory pain maintenance.

AMPARs can also contribute to glutamate-mediated signaling at non-synaptic locations. Strong primary afferent inputs generated from peripheral nociceptors by persistent inflammation may produce glutamate spillover from nearby primary afferent terminals [30]. In addition, excessive glutamate is released from glia during dorsal horn injuries or inflammation [2,30,56]. This endogenously released glutamate may activate not only post-synaptic AMPARs [45] but also extrasynaptic glutamate receptors. The latter may further strengthen glutamatergic transmission under persistent inflammatory conditions.

4.4 Tonic excitatory SG neurons likely contribute to the maintenance of inflammatory pain

Peripheral inflammation alters AMPAR trafficking in the SG neurons characterized by intrinsic tonic firing properties, but not in those that exhibit strong adaptation. In the transient neurons, CFA injection did not change the amplitudes of AMPA-induced current and associated $[Ca^{2+}]_i$ transients 24 h post-injection (Fig. 4). Taking into account that AMPA-induced current and $[Ca^{2+}]_i$ transients did not differ between tonic and transient neurons from the saline-treated group, we suggest that the total receptor pool is stable in the transient neurons even at the peak of inflammation. Our cobalt staining results also showed that a proportion of NeuN-marked neurons in superficial dorsal horn 24 h post-CFA were not cobalt-positive (Fig. 2). Thus, it is evident that inflammation-induced changes in AMPAR trafficking occur specifically in a subpopulation of SG neurons. It is known that the population of SG neurons is not homogeneous and displays distinct immunohistochemical [18,29], electrophysiological [5,20,21], and functional properties. The superficial dorsal horn neurons are characterized by different patterns of AMPAR subunit expression [18,29]. Under normal conditions, surface GluR1 protein expression is particularly associated with inhibitory dorsal horn neurons, whereas GluR2, mainly observed in this work, is associated with excitatory neurons [1,29]. Furthermore, in the SG, most tonic interneurons are excitatory [46]. These neurons make synaptic connections not only within lamina II, but also in lamina I, a region where the most nociceptive projection neurons are localized [12,33,34]. It is therefore reasonable to conclude that altered AMPAR trafficking in excitatory tonic SG neurons might be a key component in spinal central sensitization that underlies the maintenance of persistent inflammatory pain.

NIH-PA Author Manuscript

NIH-PA Author Manuscript

NIH-PA Author Manuscript

In conclusion, our study has shown that CFA-induced peripheral inflammation increases the number of extrasynaptic Ca^{2+}-permeable AMPARs as well as their proportion within the entire pool of extrasynaptic AMPARs in tonically firing SG neurons during the maintenance period. Thus, tonically firing SG neurons may represent a specific population of spinal neurons that carry out nociceptive inputs and contribute to spinal central sensitization. Since the total amount of GluR1 remains constant under CFA-induced inflammatory pain conditions [42], the observed increase in extrasynaptic Ca^{2+}-permeable AMPARs is likely attributable to CFA-promoted GluR1 membrane insertion at extrasynaptic membranes. Although the molecular mechanisms that underlie this GluR1 trafficking are still unclear, our study suggests that extrasynaptic GluR1-containing Ca^{2+}-permeable AMPARs in the dorsal horn may be used as a new target in preventing and treating persistent inflammatory pain.

Acknowledgments

This work was supported by NASU Biotechnology and INTAS 8061 grants (N.V.), NIH Grant NS058886, Mr. David Koch and the Patrick C. Walsh Prostate Cancer Research Fund, and the Johns Hopkins University Blaustein Pain Research Fund (Y.X.T), and the Intramural Research Program of NIDCD (R.S.P.). We thank Mrs. Ya-Xian Wang for help with the immunogold experiments. The authors thank Claire F. Levine, MS, for her editorial assistance.

References

1. Albuquerque C, Lee CJ, Jackson AC, MacDermott AB. Subpopulations of GABAergic and non-GABAergic rat dorsal horn neurons express Ca2+-permeable AMPA receptors. Eur J Neurosci. 1999; 11:2758–2766. [PubMed: 10457172]
2. Allan SM, Rothwell NJ. Cytokines and acute neurodegeneration. Nat Rev Neurosci. 2001; 2:734–744. [PubMed: 11584311]
3. Arendt KL, Royo M, Fernandez-Monreal M, Knafo S, Petrok CN, Martens JR, Esteban JA. PIP3 controls synaptic function by maintaining AMPA receptor clustering at the postsynaptic membrane. Nat Neurosci. 2010; 13:36–44. [PubMed: 20010819]
4. Atianjoh FE, Yaster M, Zhao X, Takamiya K, Xia J, Gauda EB, Huganir RL, Tao YX. Spinal cord protein interacting with C kinase 1 is required for the maintenance of complete Freund's adjuvant-induced inflammatory pain but not for incision-induced post-operative pain. Pain. 2010; 151:226–234. [PubMed: 20696523]
5. Balasubramanyan S, Stemkowski PL, Stebbing MJ, Smith PA. Sciatic chronic constriction injury produces cell-type-specific changes in the electrophysiological properties of rat substantia gelatinosa neurons. J Neurophysiol. 2006; 96:579–590. [PubMed: 16611846]
6. Beique JC, Huganir RL. AMPA receptor subunits get their share of the pie. Neuron. 2009; 62:165–168. [PubMed: 19409261]
7. Borgdorff AJ, Choquet D. Regulation of AMPA receptor lateral movements. Nature. 2002; 417:649–653. [PubMed: 12050666]
8. Bredt DS, Nicoll RA. AMPA receptor trafficking at excitatory synapses. Neuron. 2003; 40:361–379. [PubMed: 14556714]
9. Brown KM, Wrathall JR, Yasuda RP, Wolfe BB. Quantitative measurement of glutamate receptor subunit protein expression in the postnatal rat spinal cord. Brain Res Dev Brain Res. 2002; 137:127–133.
10. Buldakova SL, Kim KK, Tikhonov DB, Magazanik LG. Selective blockade of Ca2+ permeable AMPA receptors in CA1 area of rat hippocampus. Neuroscience. 2007; 144:88–99. [PubMed: 17097234]
11. Burnashev N, Monyer H, Seeburg PH, Sakmann B. Divalent ion permeability of AMPA receptor channels is dominated by the edited form of a single subunit. Neuron. 1992; 8:189–198. [PubMed: 1370372]
12. Burstein R, Cliffer KD, Giesler GJ Jr. Direct somatosensory projections from the spinal cord to the hypothalamus and telencephalon. J Neurosci. 1987; 7:4159–4164. [PubMed: 3694268]

NIH-PA Author Manuscript NIH-PA Author Manuscript NIH-PA Author Manuscript

13. Carroll RC, Lissin DV, von ZM, Nicoll RA, Malenka RC. Rapid redistribution of glutamate receptors contributes to long-term depression in hippocampal cultures. Nat Neurosci. 1999; 2:454–460. [PubMed: 10321250]
14. Choi JI, Svensson CI, Koehrn FJ, Bhuskute A, Sorkin LS. Peripheral inflammation induces tumor necrosis factor dependent AMPA receptor trafficking and Akt phosphorylation in spinal cord in addition to pain behavior. Pain. 2010; 149:243–253. [PubMed: 20202754]
15. Choquet D, Triller A. The role of receptor diffusion in the organization of the postsynaptic membrane. Nat Rev Neurosci. 2003; 4:251–265. [PubMed: 12671642]
16. Cognet L, Groc L, Lounis B, Choquet D. Multiple routes for glutamate receptor trafficking: surface diffusion and membrane traffic cooperate to bring receptors to synapses. Sci STKE. 2006; 2006:e13.
17. Derkach VA, Oh MC, Guire ES, Soderling TR. Regulatory mechanisms of AMPA receptors in synaptic plasticity. Nat Rev Neurosci. 2007; 8:101–113. [PubMed: 17237803]
18. Engelman HS, Allen TB, MacDermott AB. The distribution of neurons expressing calcium-permeable AMPA receptors in the superficial laminae of the spinal cord dorsal horn. J Neurosci. 1999; 19:2081–2089. [PubMed: 10066261]
19. Ferguson AR, Christensen RN, Gensel JC, Miller BA, Sun F, Beattie EC, Bresnahan JC, Beattie MS. Cell death after spinal cord injury is exacerbated by rapid TNF alpha-induced trafficking of GluR2-lacking AMPARs to the plasma membrane. J Neurosci. 2008; 28:11391–11400. [PubMed: 18971481]
20. Graham BA, Brichta AM, Callister RJ. In vivo responses of mouse superficial dorsal horn neurones to both current injection and peripheral cutaneous stimulation. J Physiol. 2004; 561:749–763. [PubMed: 15604230]
21. Grudt TJ, Perl ER. Correlations between neuronal morphology and electrophysiological features in the rodent superficial dorsal horn. J Physiol. 2002; 540:189–207. [PubMed: 11927679]
22. Guire ES, Oh MC, Soderling TR, Derkach VA. Recruitment of calcium-permeable AMPA receptors during synaptic potentiation is regulated by CaM-kinase I. J Neurosci. 2008; 28:6000–6009. [PubMed: 18524905]
23. Hartmann B, Ahmadi S, Heppenstall PA, Lewin GR, Schott C, Borchardt T, Seeburg PH, Zeilhofer HU, Sprengel R, Kuner R. The AMPA receptor subunits GluR-A and GluR-B reciprocally modulate spinal synaptic plasticity and inflammatory pain. Neuron. 2004; 44:637–650. [PubMed: 15541312]
24. Heine M, Groc L, Frischknecht R, Beique JC, Lounis B, Rumbaugh G, Huganir RL, Cognet L, Choquet D. Surface mobility of postsynaptic AMPARs tunes synaptic transmission. Science. 2008; 320:201–205. [PubMed: 18403705]
25. Ho MT, Pelkey KA, Topolnik L, Petralia RS, Takamiya K, Xia J, Huganir RL, Lacaille JC, McBain CJ. Developmental expression of Ca2+-permeable AMPA receptors underlies depolarization-induced long-term depression at mossy fiber CA3 pyramid synapses. J Neurosci. 2007; 27:11651–11662. [PubMed: 17959808]
26. Hollmann M, O'Shea-Greenfield A, Rogers SW, Heinemann S. Cloning by functional expression of a member of the glutamate receptor family. Nature. 1989; 342:643–648. [PubMed: 2480522]
27. Jones TL, Sorkin LS. Activated PKA and PKC, but not CaMKIIalpha, are required for AMPA/Kainate-mediated pain behavior in the thermal stimulus model. Pain. 2005; 117:259–270. [PubMed: 16150547]
28. Katano T, Furue H, Okuda-Ashitaka E, Tagaya M, Watanabe M, Yoshimura M, Ito S. N-ethylmaleimide-sensitive fusion protein (NSF) is involved in central sensitization in the spinal cord through GluR2 subunit composition switch after inflammation. Eur J Neurosci. 2008; 27:3161–3170. [PubMed: 18598260]
29. Kerr RC, Maxwell DJ, Todd AJ. GluR1 and GluR2/3 subunits of the AMPA-type glutamate receptor are associated with particular types of neurone in laminae I-III of the spinal dorsal horn of the rat. Eur J Neurosci. 1998; 10:324–333. [PubMed: 9753141]
30. Kullmann DM. Spillover and synaptic cross talk mediated by glutamate and GABA in the mammalian brain. Prog Brain Res. 2000; 125:339–351. [PubMed: 11098670]

NIH-PA Author Manuscript NIH-PA Author Manuscript NIH-PA Author Manuscript

31. Kwak S, Weiss JH. Calcium-permeable AMPA channels in neurodegenerative disease and ischemia. Curr Opin Neurobiol. 2006; 16:281–287. [PubMed: 16698262]
32. Leonoudakis D, Zhao P, Beattie EC. Rapid Tumor Necrosis Factor {alpha}-Induced Exocytosis of Glutamate Receptor 2-Lacking AMPA Receptors to Extrasynaptic Plasma Membrane Potentiates Excitotoxicity. J Neurosci. 2008; 28:2119–2130. [PubMed: 18305246]
33. Lima D. Anatomical basis for the dynamic processing of nociceptive input. Eur J Pain. 1998; 2:195–202. [PubMed: 15102379]
34. Lima D, Coimbra A. The spinothalamic system of the rat: structural types of retrogradely labelled neurons in the marginal zone (lamina I). Neuroscience. 1988; 27:215–230. [PubMed: 2462188]
35. Lu W, Shi Y, Jackson AC, Bjorgan K, During MJ, Sprengel R, Seeburg PH, Nicoll RA. Subunit Composition of Synaptic AMPA Receptors Revealed by a Single-Cell Genetic Approach. Neuron. 2009; 62:254–268. [PubMed: 19409270]
36. Lu Y, Perl ER. Modular organization of excitatory circuits between neurons of the spinal superficial dorsal horn (laminae I and II). J Neurosci. 2005; 25:3900–3907. [PubMed: 15829642]
37. Luo C, Seeburg PH, Sprengel R, Kuner R. Activity-dependent potentiation of calcium signals in spinal sensory networks in inflammatory pain states. Pain. 2008; 140:358–367. [PubMed: 18926636]
38. Malinow R, Malenka RC. AMPA receptor trafficking and synaptic plasticity. Annu Rev Neurosci. 2002; 25:103–126. [PubMed: 12052905]
39. Masugi-Tokita M, Shigemoto R. High-resolution quantitative visualization of glutamate and GABA receptors at central synapses. Current Opinion in Neurobiology. 2007; 17:387–393. [PubMed: 17499496]
40. Masugi-Tokita M, Tarusawa E, Watanabe M, Molnar E, Fujimoto K, Shigemoto R. Number and Density of AMPA Receptors in Individual Synapses in the Rat Cerebellum as Revealed by SDS-Digested Freeze-Fracture Replica Labeling. J Neurosci. 2007; 27:2135–2144. [PubMed: 17314308]
41. Park JS, Voitenko N, Petralia RS, Guan X, Xu JT, Steinberg JP, Takamiya K, Sotnik A, Kopach O, Huganir RL, Tao YX. Persistent inflammation induces GluR2 internalization via NMDA receptor-triggered PKC activation in dorsal horn neurons. J Neurosci. 2009; 29:3206–3219. [PubMed: 19279258]
42. Park JS, Yaster M, Guan X, Xu JT, Shih MH, Guan Y, Raja SN, Tao YX. Role of spinal cord alpha-amino-3-hydroxy-5-methyl-4-isoxazolepropionic acid receptors in complete Freund's adjuvant-induced inflammatory pain. Mol Pain. 2008; 4:67. [PubMed: 19116032]
43. Petralia RS, Wang YX, Mayat E, Wenthold RJ. Glutamate receptor subunit 2-selective antibody shows a differential distribution of calcium-impermeable AMPA receptors among populations of neurons. J Comp Neurol. 1997; 385:456–476. [PubMed: 9300771]
44. Petrini EM, Lu J, Cognet L, Lounis B, Ehlers MD, Choquet D. Endocytic trafficking and recycling maintain a pool of mobile surface AMPA receptors required for synaptic potentiation. Neuron. 2009; 63:92–105. [PubMed: 19607795]
45. Russo RE, Delgado-Lezama R, Hounsgaard J. Dorsal root potential produced by a TTX-insensitive micro-circuitry in the turtle spinal cord. J Physiol. 2000; 528(Pt 1):115–122. [PubMed: 11018110]
46. Santos SF, Rebelo S, Derkach VA, Safronov BV. Excitatory interneurons dominate sensory processing in the spinal substantia gelatinosa of rat. J Physiol. 2007; 581:241–254. [PubMed: 17331995]
47. Shi SH, Hayashi Y, Petralia RS, Zaman SH, Wenthold RJ, Svoboda K, Malinow R. Rapid spine delivery and redistribution of AMPA receptors after synaptic NMDA receptor activation. Science. 1999; 284:1811–1816. [PubMed: 10364548]
48. Singh OV, Yaster M, Xu JT, Guan Y, Guan X, Dharmarajan AM, Raja SN, Zeitlin PL, Tao YX. Proteome of synaptosome-associated proteins in spinal cord dorsal horn after peripheral nerve injury. Proteomics. 2009; 9:1241–1253. [PubMed: 19206110]
49. Sommer B, Keinanen K, Verdoorn TA, Wisden W, Burnashev N, Herb A, Kohler M, Takagi T, Sakmann B, Seeburg PH. Flip and flop: a cell-specific functional switch in glutamate-operated channels of the CNS. Science. 1990; 249:1580–1585. [PubMed: 1699275]

NIH-PA Author Manuscript

NIH-PA Author Manuscript

NIH-PA Author Manuscript

50. Tao YX. Dorsal horn alpha-amino-3-hydroxy-5-methyl-4-isoxazolepropionic acid receptor trafficking in inflammatory pain. Anesthesiology. 2010; 112:1259–1265. [PubMed: 20395828]
51. Tao YX, Rumbaugh G, Wang GD, Petralia RS, Zhao C, Kauer FW, Tao F, Zhuo M, Wenthold RJ, Raja SN, Huganir RL, Bredt DS, Johns RA. Impaired NMDA receptor-mediated postsynaptic function and blunted NMDA receptor-dependent persistent pain in mice lacking postsynaptic density-93 protein. J Neurosci. 2003; 23:6703–6712. [PubMed: 12890763]
52. Tong CK, MacDermott AB. Both Ca2+-permeable and -impermeable AMPA receptors contribute to primary synaptic drive onto rat dorsal horn neurons. J Physiol. 2006; 575:133–144. [PubMed: 16763002]
53. Triller A, Choquet D. New concepts in synaptic biology derived from single-molecule imaging. Neuron. 2008; 59:359–374. [PubMed: 18701063]
54. Vikman KS, Rycroft BK, Christie MJ. Switch to Ca2+-permeable AMPA and reduced NR2B NMDA receptor-mediated neurotransmission at dorsal horn nociceptive synapses during inflammatory pain in the rat. J Physiol. 2008; 586:515–527. [PubMed: 18033811]
55. Voitenko N, Gerber G, Youn D, Randic M. Peripheral inflamation-induced increase of AMPA-mediated currents and Ca2+ transients in the presence of cyclothiazide in the rat substantia gelatinosa neurons. Cell Calcium. 2004; 35:461–469. [PubMed: 15003855]
56. Weng HR, Chen JH, Cata JP. Inhibition of glutamate uptake in the spinal cord induces hyperalgesia and increased responses of spinal dorsal horn neurons to peripheral afferent stimulation. Neuroscience. 2006; 138:1351–1360. [PubMed: 16426766]
57. Youn DH, Voitenko N, Gerber G, Park YK, Galik J, Randic M. Altered long-term synaptic plasticity and kainate-induced Ca2+ transients in the substantia gelatinosa neurons in GLU(K6)-deficient mice. Brain Res Mol Brain Res. 2005; 142:9–18. [PubMed: 16219388]

NIH-PA Author Manuscript

NIH-PA Author Manuscript

NIH-PA Author Manuscript

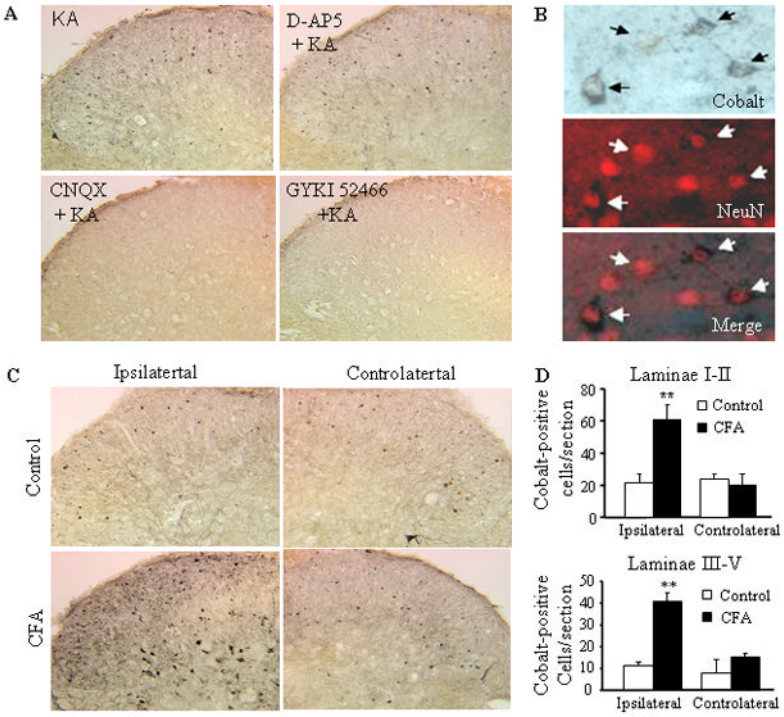

Fig. 1.

Increased kainate-induced cobalt loading in the dorsal horn after CFA injection. (A) Representative examples of kainate-induced cobalt loading in live spinal cord slices in the absence or presence of the NMDA receptor antagonist APV (500 μM) or AMPAR antagonists CNQX (250 μM) and GYKI 52466 (250 μM). (B) The neuronal marker NeuN overlaps with cobalt-uptake in the superficial dorsal horn. (C) CFA (but not saline) injection increased cobalt uptake in dorsal horn neurons on the ipsilateral, but not contralateral, side. (D) Statistical summary of the number of cobalt-positive dorsal horn neurons in laminae I-II (top graph) and laminae III-VII (bottom graph) 24 h after saline and CFA.

NIH-PA Author Manuscript

NIH-PA Author Manuscript

NIH-PA Author Manuscript

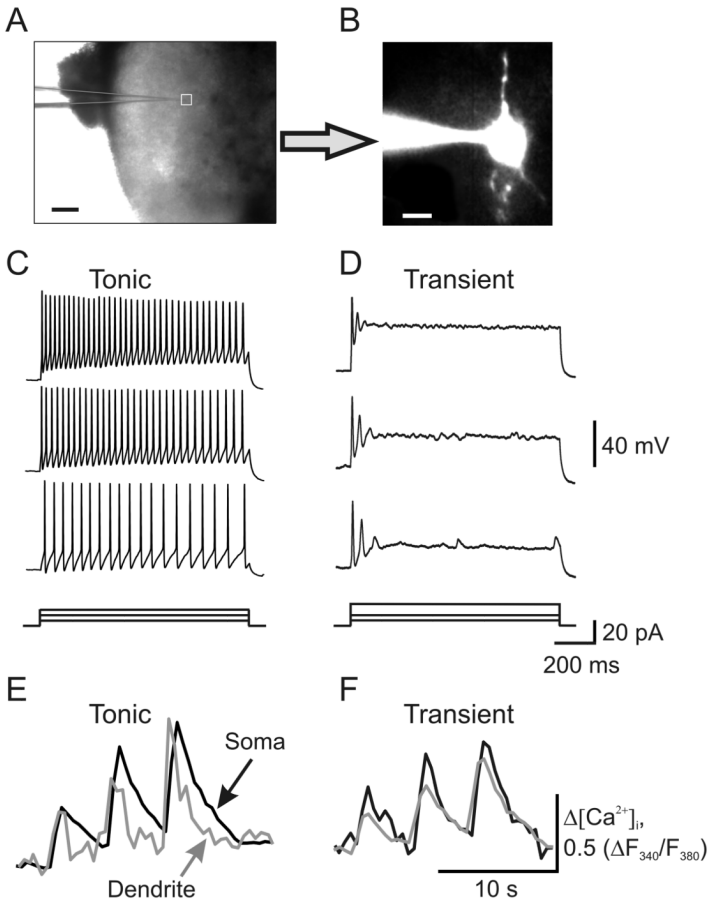

Fig. 2.

Sustained membrane depolarization revealed two groups of SG neurons exhibiting different discharge patterns. (A) Transmitted light image of patch electrode position (square) in the SG of a transverse dorsal horn slice; scale bar = 200 μm. (B) A fluorescent image of a neuron loaded with fura-2 (200 μM); scale bar = 20 μm. (C, D) Current-clamp recordings of typical firing patterns for tonic (C) and transient (D) groups of neurons in response to three different intensities of depolarizing currents shown at the bottom of each panel. (E, F) Recordings of depolarizing current-induced changes in the cytosolic free calcium concentration ($[Ca^{2+}]_i$) in the soma (black traces) and dendrites (grey traces) in tonic (E) and transient (F) groups of neurons.

NIH-PA Author Manuscript

NIH-PA Author Manuscript

NIH-PA Author Manuscript

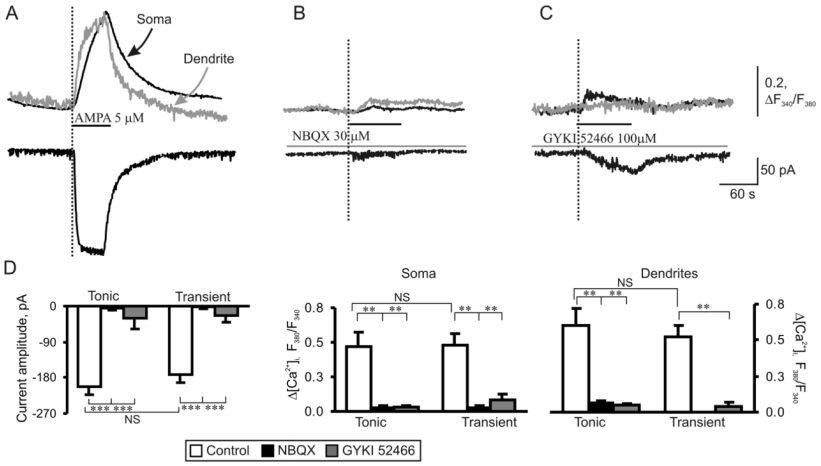

Fig. 3.

AMPAR-mediated currents and $[Ca^{2+}]_i$ transients are similar in tonic and transient neurons of naive rats. (A) Representative traces of a somatic membrane current (bottom trace) and associated $[Ca^{2+}]_i$ transients (upper traces) recorded from the soma (black trace) and dendrites (grey trace) in tonic neurons during AMPA bath application (5 μM, 60 s). (B, C) Pre-application of AMPAR antagonists NBQX (30 μM, B) and GYKI 52466 (100 μM, C) abolished AMPA-induced current (lower traces) and associated somatic (upper black traces) and dendritic (upper grey traces) $[Ca^{2+}]_i$ transients. (D) Pooled results demonstrate that AMPA-induced current amplitudes (left graph) and $[Ca^{2+}]_i$ transients (center and right graphs) recorded from soma and dendrites of different groups of SG neurons are similar. ** $p < 0.001$, *** $p < 0.0001$ versus the control; NS, not significant.

NIH-PA Author Manuscript

NIH-PA Author Manuscript

NIH-PA Author Manuscript

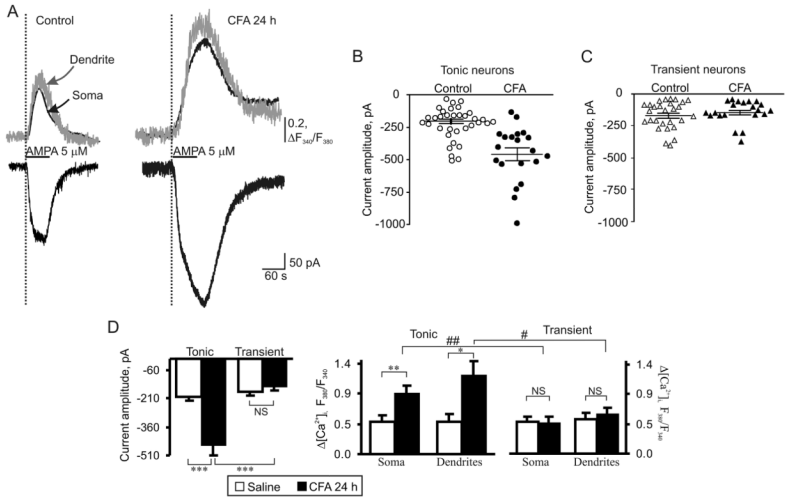

Fig. 4.

AMPAR-mediated currents and associated $[Ca^{2+}]_i$ transients are markedly potentiated in tonic but not in transient SG neurons during persistent inflammation. (A) Representative examples of AMPA-induced currents (lower traces) and $[Ca^{2+}]_i$ transients (upper traces) in soma (black traces) and dendrites (grey traces) in tonic neurons 24 h after saline (control) or CFA. (B, C) Scatter dot plots illustrate a spread in extrasynaptic AMPAR-mediated currents in tonic (B) and transient (C) neurons 24 h after saline or CFA. (D) A statistical summary of current amplitudes (left graph) and $[Ca^{2+}]_i$ transients (right two graphs) in soma and dendrites of different groups of SG neurons 24 h post-saline and post-CFA. * $p < 0.05$, ** $p < 0.001$, *** $p < 0.0001$ versus the saline-treated group; # $p < 0.05$, ## $p < 0.001$ versus the transient SG neurons; NS, not significant.

NIH-PA Author Manuscript

NIH-PA Author Manuscript

NIH-PA Author Manuscript

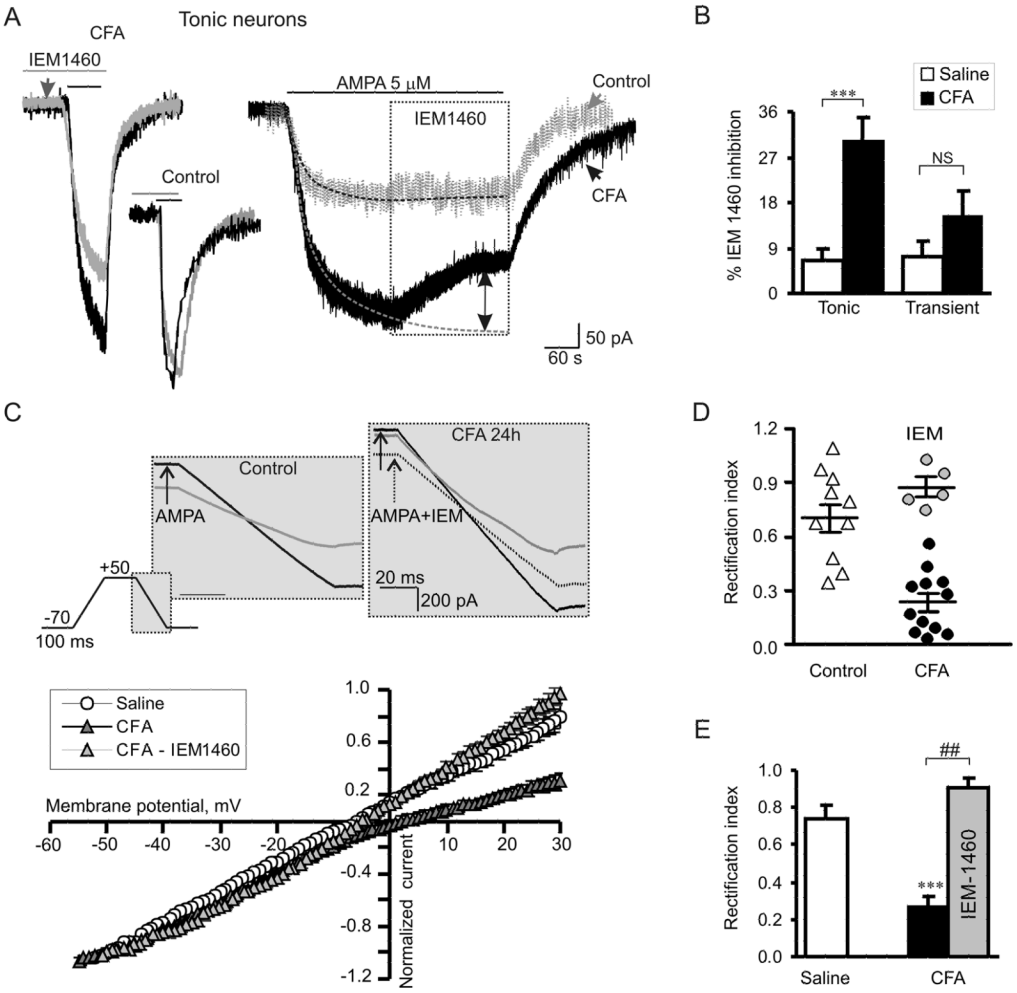

Fig. 5.

Persistent peripheral inflammation increases the proportion of Ca^{2+}-permeable AMPARs in the extrasynaptic plasma membrane of tonic SG neurons. (A) A selective blocker of Ca^{2+}-permeable AMPARs, IEM-1460 (40 μM), substantially inhibited AMPA-induced currents in tonic neurons of CFA-treated but not of saline-treated rats. Left, an overlay of AMPA-induced currents recorded in the absence (black traces) and presence (pre-incubation for 5 min; grey traces) of IEM-1460 24 h after saline or CFA. Right, IEM-1460 was bath applied during a steady-state phase of AMPA-induced current. Dotted lines represent exponential fitting of the currents; dotted arrow indicates the value of IEM-1460 inhibition. (B) A statistical summary of IEM-1460 inhibition of extrasynaptic AMPARs in tonic and transient SG neurons. *** $p < 0.0001$ versus the saline-treated group. (C) The top panel illustrates the protocol for reconstruction of the *I-V* relationship from ramp recordings. The bottom panel shows *I-V* curves obtained in tonic neurons at 24 h post-saline or post-CFA. Note that IEM-1460 reverses the rectification of AMPA-induced currents recorded from neurons of CFA-treated rats. (D, E) The scatter plot illustrates the spread in rectification index (RI = I_{+30mV}/I_{-50mV}) (D), and the bar graph shows the statistical summary for RI (E) in tonic neurons 24 h post-saline and post-CFA before (black) and after (grey) IEM-1460 application. *** $p < 0.0001$ versus the saline-treated group, ## $p < 0.001$ versus the CFA-treated group.

NIH-PA Author Manuscript

NIH-PA Author Manuscript

NIH-PA Author Manuscript

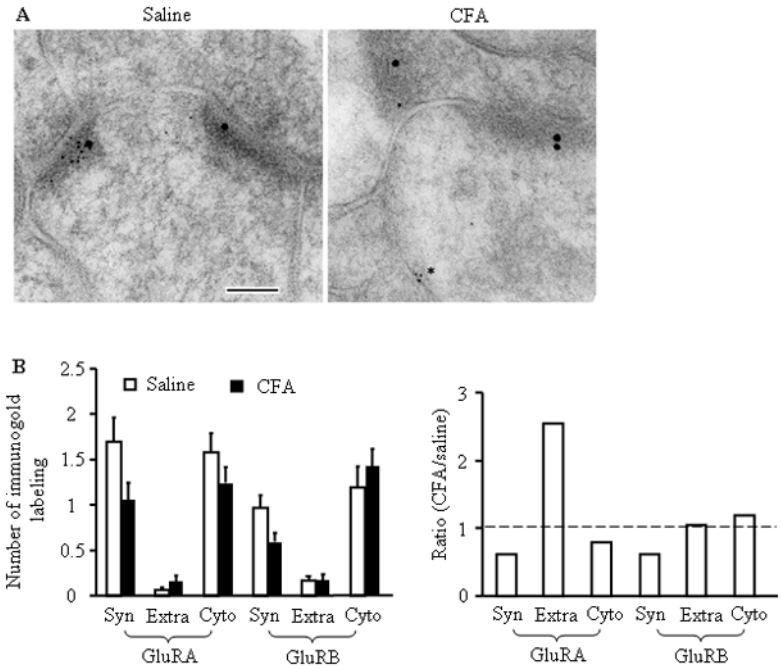

Fig. 6.

Ultrastructural distribution of GluR1 and GluR2 in the superficial dorsal horn 24 h after saline (left) or CFA (right) injection. (A) Representative micrographs of postembedding immunogold labeling for GluR1 (5 nm) and GluR2 (15 nm). In these representative images, the synapses are marked by the presence of GluR2; GluR1 is more prevalent at synapses in the saline-treated group. In the CFA-treated group, GluR1 is evident in the extrasynaptic membrane (asterisk). PSD, postsynaptic density; pre, presynaptic terminal; scale bar = 100 nm. (B) The left bar graph shows the number of GluR1- and GluR2-labeled immunogold particles at synapses (Syn), at extrasynaptic membranes (Extra), and in cytoplasm (Cyto) of superficial dorsal horn neurons 24 h after CFA or saline injection. The right bar graph shows ratios of the number of GluR1- and GluR2-labeled particles in the CFA-treated group to those in the saline-treated group at synapses, extrasynaptic membranes, and cytoplasm of superficial dorsal horn neurons 24 h after injections.

NIH-PA Author Manuscript

NIH-PA Author Manuscript

NIH-PA Author Manuscript

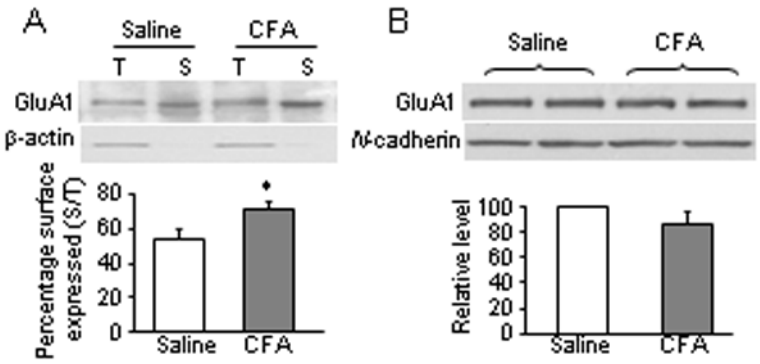

Fig. 7.

GluR1 membrane insertion in dorsal horn neurons 24 h after CFA injection. (A) Surface expression of GluR1 in dorsal horn neurons 24 h after CFA or saline injection. Top, representative Western blot; bottom, statistical summary of the densitometric analysis. The level of sample loaded for the total (T) expression was 10% of that for the biotinylated surface (S) expression. * $p < 0.05$ versus the saline-treated group. β-actin, an unbiotinylated intracellular protein, was used as a control. (B) Expression of GluR1 in the synaptosomal fraction from dorsal horn 1 day after CFA or saline injection. Top, representative Western blot; bottom, statistical summary of the densitometric analysis. *N*-cadherin, a membrane marker, was used as a control.